# Soluble RAGE Prevents Type 1 Diabetes Expanding Functional Regulatory T Cells

Sherman S. Leung,[1,2] Danielle J. Borg,[1,3] Domenica A. McCarthy,[1] Tamar E. Boursalian,[4] Justen Cracraft,[4] Aowen Zhuang,[1] Amelia K. Fotheringham,[1,2] Nicole Flemming,[1,2] Thomas Watkins,[5] John J. Miles,[5] Per-Henrik Groop,[6–9] Jean L. Scheijen,[10,11] Casper G. Schalkwijk,[10,11] Raymond J. Steptoe,[12] Kristen J. Radford,[2,13] Mikael Knip,[6,14] and Josephine M. Forbes[1,9,15]

*Diabetes 2022;71:1994–2008 | https://doi.org/10.2337/db22-0177*

**Type 1 diabetes is an autoimmune disease with no cure, where clinical translation of promising therapeutics has been hampered by the reproducibility crisis. Here, short-term administration of an antagonist to the receptor for advanced glycation end products (sRAGE) protected against murine diabetes at two independent research centers. Treatment with sRAGE increased regulatory T cells ($T_{regs}$) within the islets, pancreatic lymph nodes, and spleen, increasing islet insulin expression and function. Diabetes protection was abrogated by $T_{reg}$ depletion and shown to be dependent on antagonizing RAGE with use of knockout mice. Human $T_{regs}$ treated with a RAGE ligand downregulated genes for suppression, migration, and $T_{reg}$ homeostasis (*FOXP3*, *IL7R*, *TIGIT*, *JAK1*, *STAT3*, *STAT5b*, *CCR4*). Loss of suppressive function was reversed by sRAGE, where $T_{regs}$ increased proliferation and suppressed conventional T-cell division, confirming that sRAGE expands functional human $T_{regs}$. These results highlight sRAGE as an attractive treatment to prevent diabetes, showing efficacy and reproducibility at multiple research centers and in human T cells.**

Type 1 diabetes (T1D) is an autoimmune disease involving a heterogeneous interplay between genetic and environmental factors resulting in T cell–mediated destruction of insulin-producing β-cells (1). T1D incidence is increasing at 2–3% per year worldwide, elevating the risk for premature death and costing $14 billion per annum in health care in the U.S. (2). Risk factors for developing T1D include decreases in functional regulatory T cells ($T_{regs}$) (3) and increased numbers of autoantigen-specific conventional T cells ($T_{convs}$), particularly effector phenotypes ($T_{eff}$) (4). Early-phase clinical trials promoting $T_{reg}$ expansion, thereby suppressing $T_{conv}$ activation, have shown promise in preserving insulin production after diagnosis of T1D (5,6), but findings await validation in larger cohorts. However, interventions aimed at reversing clinically diagnosed T1D may be "too late," with phase III clinical trials not reaching primary end points (7). As a result, promising therapeutics targeting T cells are being repurposed for use in prediabetes (7) to prevent onset of T1D (clinical trial reg. nos. NCT01030861 and NCT01773707, ClinicalTrials.gov). Indeed, in the former, a phase II randomized study, it was reported that

[1]Glycation and Diabetes, Mater Research, The University of Queensland and Translational Research Institute, Brisbane, Australia
[2]School of Biomedical Sciences, The University of Queensland, Brisbane, Australia
[3]Inflammatory Disease Biology and Therapeutics, Mater Research, The University of Queensland and Translational Research Institute, Brisbane, Australia
[4]Type 1 Diabetes Research Center, Novo Nordisk, Seattle, WA
[5]Centre for Biodiscovery and Molecular Development of Therapeutics, Australian Institute of Tropical Health and Medicine, James Cook University, Cairns, Australia
[6]Research Program for Clinical and Molecular Metabolism, Faculty of Medicine, University of Helsinki, Helsinki, Finland
[7]Folkhälsan Research Center, Helsinki, Finland
[8]Nephrology, Abdominal Center, University of Helsinki and Helsinki University Hospital, Helsinki, Finland
[9]Baker IDI Heart and Diabetes Institute, Melbourne, Australia
[10]Laboratory for Metabolism and Vascular Medicine, Department of Internal Medicine, Maastricht University, Maastricht, the Netherlands
[11]Cardiovascular Research Institute Maastricht, Maastricht, the Netherlands
[12]Diamantina Institute, The University of Queensland and Translational Research Institute, Brisbane, Australia
[13]Cancer Immunotherapies, Mater Research, The University of Queensland and Translational Research Institute, Brisbane, Australia
[14]Pediatric Research Center, Children's Hospital, University of Helsinki and Helsinki University Hospital, Helsinki, Finland
[15]Mater Clinical School, The University of Queensland, Brisbane, Australia

Corresponding author: Josephine M. Forbes, josephine.forbes@mater.uq.edu.au

Received 24 February 2022 and accepted 23 May 2022

This article contains supplementary material online at https://doi.org/10.2337/figshare.20051633.





PATHOPHYSIOLOGY

teplizumab—an Fc receptor nonbinding anti-CD3 monoclonal antibody—significantly delayed onset of T1D (8). Thus, interventions delivered for prediabetes are clinically feasible, have a greater chance of preserving insulin secretion, and could prevent onset of T1D.

The receptor for advanced glycation end products (RAGE) is a pattern recognition receptor implicated in inflammatory diseases and is expressed in various cells involved in T1D including T cells (reviewed in 9). Recently, changes in circulating (termed soluble) RAGE concentrations have been associated with risk for developing T1D in humans (10–12). Furthermore, T cells from individuals at risk who progress to T1D have greater RAGE expression, which enhances T-cell cytokine production and survival (13). Natural history studies have further revealed that polymorphisms in the RAGE gene (*AGER*), which decrease circulating soluble RAGE (sRAGE) concentrations (12), a naturally occurring antagonist that competes for RAGE ligands, increase the risk of T1D (14). These decreases in circulating sRAGE also coincide with seroconversion to autoantibodies against islet autoantigens in individuals at risk (10,11). Therefore, this deficiency in circulating sRAGE presents a novel therapeutic target for preventing the onset of T1D.

In the current study, we targeted the deficiency in circulating sRAGE concentrations in prediabetes with short-term administration of recombinant human sRAGE with the aim of preventing diabetes onset in mice. sRAGE acted in an immunomodulatory manner to decrease diabetes incidence at two independent research centers, increasing the proportion of $T_{regs}$ in the islet-infiltrating leukocytes, pancreatic lymph nodes (PLN), and spleen, which reduced islet infiltration and preserved islet numbers, insulin expression, and β-cell function. Depletion of $T_{regs}$ in adoptively transferred diabetes reversed the capacity of sRAGE to prevent T1D and sRAGE administration to wild-type but not RAGE knockout (KO) mice increased $T_{reg}$ numbers and function. Ex vivo, sRAGE promoted the expansion of human $T_{regs}$ and reduced $T_{conv}$ proliferation in coculture, whereas $T_{regs}$ cultured in the presence of the RAGE ligand, advanced glycation end products (AGEs), had reduced suppressive function. Our data suggest that short-term delivery of sRAGE effectively modulates functional $T_{reg}$ expansion, thereby preventing diabetes and potentially other autoimmune disease.

## RESEARCH DESIGN AND METHODS

### Murine Incidence Studies

For the incidence analyses, female NOD/ShiLt mice were housed in specific pathogen-free conditions at two independent research centers: site 1, Translational Research Institute, and site 2, Type 1 Diabetes Research Center, Novo Nordisk. Mice were sourced from The Animal Resources Centre (Canning Vale, Australia [site 1]) or The Jackson Laboratory (Sacramento, CA [site 2]) and provided free access to irradiated diet (site 1, Specialty Feeds Rat and Mouse Diet; site 2, Purina LabDiet 5053) and water (site 1, autoclaved; site 2, filtered). Randomized mice were intraperitoneally injected on days 50–64 of life with 100 μL recombinant human sRAGE (25 μg) twice daily (sites 1 and 2), vehicle (PBS) twice daily (site 1), or sRAGE (100 μg) once daily (site 2) or were untreated (site 2). Mice were fasted for 4–6 h and euthanized on day 64 or 80 or, for nonprogressors, day 225 of life. Nonfasted blood glucose concentrations were measured weekly with a glucometer (site 1, SensoCard; site 2, Bayer CONTOUR USB) between days 50 and 225. Diabetes was diagnosed when this exceeded 15 mmol/L on consecutive days, at which point these progressors left the study.

For all other study analyses, female NOD/SCIDs, wild-type C57BL/6, and RAGE KO C57BL/6 (15) mice were housed at site 1. Animal studies were approved at both sites by their respective institutional ethics committees and adhered to national guidelines by the National Health and Medical Research Council (NHMRC) (Australia) and National Institutes of Health (U.S.).

### Adoptive Transfer of Diabetes in Mice

Splenocytes ($10^7$) from untreated female NOD/ShiLt mice diagnosed with diabetes within 7 days were injected (200 μL i.v.) into 5- to 9-week-old female NOD/SCID recipients (16). Splenocytes were mechanically dissociated with use of 70-μm filters, red cell lysis was performed with Ammonium-Chloride-Potassium (ACK) Lysing Buffer (Thermo Fisher Scientific), and splenocytes were washed several times into serum-free mouse-tonicity PBS for injection in vivo. Randomized NOD/SCID mice were then administered the following treatments 2 weeks post–adoptive transfer: *1*) PBS and rat isotype control IgG2b antibodies (RTK4530; BioLegend), *2*) PBS and anti–folate receptor 4 (FR4) antibodies (TH6; BioLegend) for the depletion of $T_{regs}$ via their selective expression of FR4 (17), *3*) sRAGE and isotype control antibodies, or *4*) sRAGE and anti-FR4 antibodies. PBS and sRAGE (25 μg) were given twice daily as described above. Isotype control and anti-FR4 antibodies (10 μg for both) were given on days 0, 3, 7, 10, and 14, and endotoxin levels were $<0.01$ endotoxin units (EU)/μg ($<0.1$ EU/injection) as determined by limulus amebocyte lysate (LAL) assay. Diabetes was monitored and diagnosed as described above.

### Islet Histology and Immunofluorescence Staining

Formalin-fixed tissue sections (4–5 μm) were deparaffinized, rehydrated, stained with hematoxylin-eosin (H-E), and imaged (VS1200 brightfield microscope; Olympus Corporation, Japan). Islet infiltration was assessed in a blinded fashion with use of an islet infiltration index from 0 to 1 as previously described (18).

For tissue immunofluorescence, antigen retrieval was performed with sodium citrate buffer (pH 6), nonspecific blocking with 10% donkey serum, and incubation with

rabbit anti-CD3 (SP7; Abcam), goat anti-CD4 (no. AF554; R&D Systems), and biotinylated anti-FoxP3 (FJK-16s; eBioscience) antibodies overnight at 4°C. This was followed by incubation with anti-rabbit IRDye 800CW (no. 926-32213; LI-COR), anti-goat Alexa Fluor 568 (no. A-11057; Thermo Fisher Scientific), and streptavidin–Alexa Fluor 647 (no. S32357; Thermo Fisher Scientific) at room temperature for 1 h. Sections were blocked as described above and then incubated with rat anti-insulin antibody (182410; R&D Systems) overnight at 4°C, followed by anti-rat Alexa Fluor 488 (no. A21208) at room temperature for 1 h. Sections were mounted with Fluoroshield-DAPI and imaged (FV1200 confocal microscope; Olympus Life Science). Blinded quantification was performed in ImageJ, version 2.0.0. Statistical tests were performed with independent biological replicates (i.e., averaging numerous sections per mouse), and scatter plots show individual islet data points for complete visualization of the data set.

### Flow Cytometry and Cell Sorting

Mouse spleen and PLN were mechanically dissociated into single cells with use of 40-μm filters, and red cell lysis was performed with ACK buffer. Blocking was performed with anti-CD16/CD32 antibodies (BD Biosciences), and cells were stained with antibodies against CD4 (RM4-5; BD Biosciences), CD8 (53-6.7; BD Biosciences), CD11b (M1/70; BD Biosciences), CD11c (HL3; BD Biosciences), B220 (RA3-6B2; BD Biosciences), F4/80 (CI:A3-1; Bio-Rad Laboratories), CD62L (MEL-14; BD Biosciences), CD44 (IM7; BD Biosciences), CD25 (PC61; BD Biosciences), FoxP3 (FJK-16s; eBioscience), TIGIT (1G9; BioLegend), KLRG1 (2F1; BioLegend) and Ki67 (16A8; BioLegend). Samples were analyzed on the LSRII (BD Biosciences) and FlowJo (Tree Star, Inc.).

### Soluble RAGE Manufacture

Recombinant sRAGE was produced from the cloned human endogenous secretory RAGE sequence in an insect cell and baculovirus expression system (referred to from here as sRAGE). Recombinant sRAGE was isolated by size exclusion and affinity chromatography and confirmed to be >99% pure with SDS-PAGE (Supplementary Fig. 1). Endotoxin levels were 0.065 EU/mg (0.00325 and 0.0065 EU/day for 25 μg twice daily and 100 μg once daily dosages, respectively) as determined with LAL assay. Treatment dosages were based on those of previous studies (19,20).

### RAGE Ligand Assays

Fasting plasma S100A8/A9 (R&D DuoSet), S100B (Abbexa), and HMGB1 (SHINO-TEST) were measured with ELISA. Circulating AGEs and dicarbonyls were measured with liquid chromatography–tandem mass spectrometry as previously described (21).

### Oral Glucose Tolerance Tests

Mice were fasted for 4–6 h and administered a 2 g/kg glucose bolus by intragastric gavage. At 0, 15, 30, 60, and 120 min post–glucose bolus, blood glucose and plasma insulin were measured by glucometer and ELISA (Crystal Chem), respectively.

### AGE–Human Serum Albumin Production

We produced AGE–human serum albumin (HSA) by incubating 20 mg/mL fatty acid–free, cold ethanol–precipitated HSA (Sigma-Aldrich) and 0.5 mol/L D-(+)-Glucose (Sigma-Aldrich) in HyClone PBS (GE Healthcare) for 3 months at 37°C in the dark. Solutions were placed into 10 kDa MWCO Slide-A-Lyzer Cassettes (Thermo Fisher Scientific) and dialyzed against PBS (GE Healthcare), 0.22 μm filtered, and stored at −80°C. Endotoxin was determined to be <1 EU/mL (<0.005 EU/mL at final concentrations in human cell culture experiments) by LAL assay. AGE-HSA glycation adducts were measured with liquid chromatography–tandem mass spectrometry as 646.5 μmol/L Nε-(carboxymethyl)lysine (CML), 45.3 μmol/L Nε-(carboxyethyl)lysine (CEL), and 198.4 μmol/L methylglyoxal-derived hydroimidazolone (MG-H1) (28-, 22-, and 11-fold increases in glycation adduct concentrations, respectively, as compared with unmodified HSA).

### Human T-Cell Culture

Human blood donors were healthy volunteers, 18–65 years of age, and provided informed consent. Experiments were approved by the Mater Human Research Ethics Committee. Fresh human peripheral blood mononuclear cells (PBMCs) were isolated with Ficoll and incubated with antibodies against CD3 (OKT3; BioLegend), CD4 (RPA-T4; Bio-Legend), CD25 (BC96; BioLegend), CD127 (A019D5; Bio-Legend), and FoxP3 (PCH101; eBioscience). Dead cells were excluded with a LIVE/DEAD viability dye (Thermo Fisher Scientific), and blocking was performed with Human TruStain FcX (BioLegend). $CD3^+CD4^+CD25^+CD127^{lo/-}$ natural $T_{regs}$ ($nT_{regs}$) and $CD3^+CD4^+CD25^-$ $T_{convs}$ were isolated on the Astrios (Beckman Coulter) or FACSAria (BD Biosciences) and analyzed with FlowJo (>97% $nT_{reg}$ and $T_{conv}$ purity). $CD3^+CD4^+CD25^+CD127^{lo/-}$ $nT_{regs}$ were 90.2 ± 7.1% FoxP3 positive (Supplementary Fig. 7*C* and *D*), consistent with previous studies (22).

Human $nT_{regs}$ were carboxyfluorescein succinimidyl ester (CFSE)-labeled and cultured in TexMACs (Miltenyi Biotec) supplemented with 10% heat-inactivated FBS (Life Technologies from here unless otherwise indicated), 100 units/mL penicillin-streptomycin, 10 μmol/L β-mercaptoethanol, and 100 μg/mL AGE-modified HSA (AGE-HSA or AGE) at a final number of $2.5 \times 10^4$ cells in a U-bottom 96-well plate. $T_{convs}$ were CellTrace Violet labeled and added at $2.5 \times 10^4$ cells/well. Cells were stimulated with anti-CD3/CD28 MACSiBeads at a 1:10 bead:cell ratio. Cocultures were treated with 50 μg sRAGE or PBS daily for 72 h at 37°C, 5% $CO_2$. Proliferation indices were analyzed with CFSE and CellTrace Violet dye dilution on the LSRFortessa (BD Biosciences) and FlowJo software proliferation gating feature.

### Human T-Cell Monoculture

CFSE-labeled human $nT_{regs}$ were also grown in monoculture with TexMACs supplemented with 10% heat-inactivated FBS, 100 units/mL penicillin-streptomycin, 10 μmol/L β-mercaptoethanol, and 200 IU/mL IL-2 at a final number of $2 \times 10^4$ cells in a U-bottom 96-well plate. Cells were stimulated with use of anti-CD3/CD28 MACSiBeads at a 1:20 bead:cell ratio and treated with 100 μg/mL HSA or AGEs for 72 h at 37°C, 5% $CO_2$, and analyzed as described above.

Naive $CD4^+$ T cells were negatively isolated from fresh PBMCs with EasySep (Stem Cell Technologies) (>95% purity). Cells were stimulated (23); treated with 100 μg/mL AGEs and 50 μg sRAGE or PBS daily for 72 h at 37°C, 5% $CO_2$; and analyzed for $CD3^+CD4^+CD25^+CD127^{lo/-}$ induced $T_{reg}$ ($iT_{reg}$) differentiation on the LSRFortessa (BD Biosciences) and FlowJo.

### Human $nT_{reg}$ Binding Assay

Human $nT_{regs}$ were stained with Hoechst 33342 (Thermo Fisher Scientific) and cultured in phenol-free RPMI-1640 (Thermo Fisher Scientific) in glass chambers and administered 100 μg/mL HSA–Alexa Fluor 488, AGE–Alexa Fluor488, or AGE–Alexa Fluor488 and anti-RAGE antibody (no. AB5484; Merck) for the durations indicated. Cells were imaged on the FV1200 confocal microscope, and quantification was performed in a blinded fashion with ImageJ.

### NanoString Analyses of Human T Cells

For gene expression analysis, unlabeled $nT_{regs}$ were grown in monoculture under the conditions described above for 72 h and anti-CD3/CD28 MACSiBeads removed with EasySep Magnet. RNA was isolated with RNAzol RT (Astral Scientific) per the manufacturer's instructions with use of molecular-grade isopropanol and ethanol (Sigma-Aldrich) for RNA precipitation. Cells were lysed and centrifuged to separate the aqueous phase that contained RNA. Multiple ethanol washes were performed before resuspension of the purified RNA pellet. RNA quality and quantity were probed with use of an Implen NanoPhotometer N60 (LabGear). RNA (100 ng) was hybridized overnight with a NanoString Custom CodeSet for 136 T cell–specific genes. Normalization of raw counts was performed with NanoString nSolver software with the housekeeping genes *ACTB*, *B2M*, *GAPDH*, *HPRT1*, and *RPLP0* (panel in Supplementary Table 3).

### Quantification and Statistical Analysis

Statistical analyses were performed with GraphPad, version 5.01, and $P < 0.05$ was considered statistically significant. Comparisons were done with biological, not technical, replicates that are shown in all figures. Normality was tested with the Kolmogorov-Smirnov test. Means were compared with two-tailed Student *t* test and are shown as means ± SD. Medians were compared with two-tailed Mann-Whitney *U* test and are shown as median (interquartile range [IQR]). Kaplan-Meier survival curves were compared with log-rank test. Regression lines were compared with ANCOVA. Proportions were compared with Fischer test. Gene expression was analyzed with R, version 3.4.4, for principal components analysis (PCA) and volcano plots; Database for Annotation, Visualization and Integrated Discovery (DAVID), version 6.8, for Reactome pathway enrichment; PANTHER, version 14.0, for gene ontology overrepresentation; and Ingenuity Pathway Analysis, version 1.14, for identification of upstream regulators and network analysis (*P* values were adjusted with false discovery rate or Bonferroni correction).

### Data and Resource Availability

The data sets generated during or analyzed in the current study are available from the corresponding author on reasonable request. The AGE-HSA in the current study is available from the corresponding author on reasonable request. The sRAGE generated in the current study is not publicly available due to ongoing drug development that is commercial and in confidence. However, sRAGE can be purchased from many vendors including ProSpec (PRO-601), BioVendor (RD172116025-HEK), and Merck (SRP6051).

## RESULTS

### Short-term sRAGE Decreases Diabetes Development at Two Geographically Distinct Sites

Recombinant human sRAGE was administered bidaily prediabetes for 2 weeks (days 50–64 of life) (Fig. 1*A*), which led to a 3.0-fold improvement in diabetes incidence by day 225 compared with vehicle-treated mice (Fig. 1*B*; site 1). Comparable results were achieved at an independent research center with greater diabetes penetrance (Fig. 1*B*; site 2), where sRAGE treatment for prediabetes at escalating dosages resulted in a 2.8-fold and 4.0-fold reduction in diabetes incidence, respectively (vs. untreated) (Fig. 1*B*).

Nonfasting blood glucose concentrations in sRAGE-treated mice were significantly lower over the study duration compared with vehicle mice (Fig. 1*C*) until approximately day 200, when both sRAGE groups had overlap (Fig. 1*C*). Blood glucose variability was also reduced following sRAGE administration (vs. vehicle/untreated) (Fig. 1*C*). From here, we characterized the effects of sRAGE at the lowest dose given bidaily.

### sRAGE Therapy Decreases Islet Infiltration and Increases Islet Numbers

Immediately after therapy completion (day 64), mice treated with sRAGE had reduced islet infiltration indices compared with vehicle (Fig. 1*D*), with a decrease in the numbers of islets with high-grade insulitis (>75% infiltrate, grade 4) and an increase in islets without insulitis (0% infiltrate, grade 0) (Fig. 1*E* and *F*). By day 80, the islet infiltration index did not differ between groups (Fig. 1*D*), and unexpectedly, sRAGE-treated mice had a modest increase in the proportion of islets with grade 4 insulitis (>75% infiltration) (Fig. 1*E* and *F*). However, by day 225, sRAGE-treated mice showed significant reduction in islet infiltration (Fig. 1*D*),

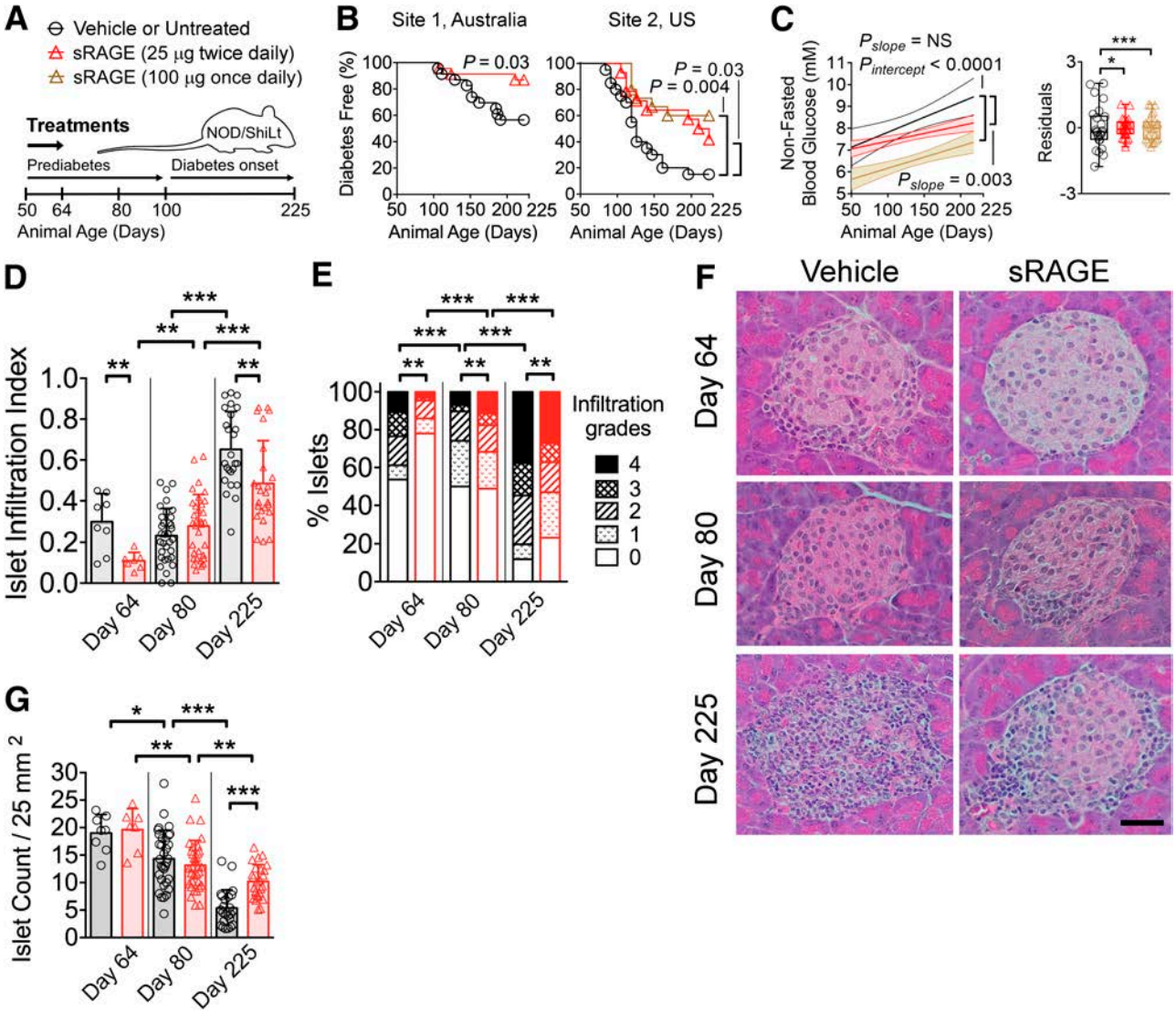


**Figure 1**—Treatment with sRAGE provides lasting protection against autoimmune diabetes in an international multisite preclinical trial. *A*: NOD/ShiLt mice were administered vehicle at site 1 or were untreated at site 2 (black bars/circles) or treated with 25 μg sRAGE twice daily (red bars/triangles) or 100 μg sRAGE once daily (brown bars/triangles) from days 50–64 of life. *B*: Autoimmune diabetes incidence. Site 1, three independent experiments, $n$ = 23/group; site 2, one independent experiment, $n$ = 14–20/group. *C*: Nonfasting blood glucose concentrations shown as linear regression ± 95% CI (left) and residuals representing variability of blood glucose levels from the regression line (right). *D–F*: Pancreatic islet infiltration. *D*: Islet infiltration index (0 indicates no infiltration; to 1 indicates >75% infiltration). *E*: Degree of islet infiltration (grade 0, none; grade 1, peri-infiltration; grade 2, <25% infiltration; grade 3, 25–75% infiltration; grade 4, >75% infiltration). *F*: Representative hematoxylin-eosin photomicrographs ($n$ = 7–33 sections/group from $n$ = 4–7 mice/group; scale bar = 40 μm). *G*: Islet count normalized by tissue area. Column graphs are shown as median (IQR), with analysis with two-tailed Mann-Whitney *U* test. Box-and-whisker plot variances were analyzed with *F* test. Degree of insulitis is shown as mean and proportions analyzed with Fischer exact test. Diabetes incidence is shown with Kaplan-Meier survival curves and was analyzed with log-rank test. *$P < 0.05$; **$P < 0.01$; ***$P < 0.001$.

increased proportion of islets without insulitis, and fewer islets scoring 4 (vs. vehicle) (Fig. 1*E* and *F*). Islet numbers decreased over the study duration in both cohorts (Fig. 1*G*), but sRAGE treatment preserved a greater number of islets by day 225 (Fig. 1*G*).

### sRAGE Rapidly Increases $T_{reg}$–to–Effector T Cell Ratios in the PLN and Spleen

Given that $T_{regs}$ in the PLN and spleen regulate islet infiltration in diabetes (24), we examined the effects of sRAGE therapy at these sites (Supplementary Fig. 2, gating strategies). Immediately after sRAGE therapy on day 64, higher numbers and proportions of $CD4^+CD8^-CD25^+Foxp3^+$ $T_{regs}$, as well as higher numbers of $FoxP3^-CD4^+$ and $FoxP3^-CD8^+$ $T_{convs}$, were observed in both the PLN and spleen (vs. vehicle) (Supplementary Fig. 3*A–C*). In the PLN, increases in $T_{reg}$ numbers elevated $T_{reg}$–to–effector T cell ($T_{eff}$) ratios in sRAGE-treated mice (Fig. 2*A–C*). Despite the increase in splenic $T_{regs}$, the ratio to $T_{eff}$ cells remained unchanged on day 64 (Fig. 2*A–C*). There was no change in the

activation status of FoxP3$^-$CD4$^+$ or FoxP3$^-$CD8$^+$ $T_{convs}$ following sRAGE treatment in either lymphoid compartments (CD62L$^+$ and CD44$^+$) (Supplementary Fig. 3*B* and *C*).

By day 225, sRAGE-treated mice had decreased numbers of CD4$^+$CD8$^-$CD25$^+$Foxp3$^+$ $T_{regs}$ and FoxP3$^-$CD8$^+$ $T_{convs}$ in the PLN and FoxP3$^-$CD4$^+$ and FoxP3$^-$CD8$^+$ $T_{convs}$ in the spleen, as compared with vehicle (Supplementary Fig. 4*A*–*C*). This suggested that there was a persistent dampening of immune responses after sRAGE treatment, which was consistent with a long-lasting increase in $T_{reg}$ frequencies in the PLN and spleen (Supplementary Fig. 4*A*) and $T_{reg}$-to-$T_{eff}$ ratios in the spleen alone (vs. vehicle) (Fig. 2*D*–*F*). The proportions of CD62L$^+$CD44$^-$ naive, CD62L$^-$CD44$^+$ effector, and CD62L$^+$CD44$^+$ memory subsets in the $T_{conv}$ populations remained unchanged between groups on day 225 (Supplementary Fig. 4*B* and *C*).

Given the importance of antigen-presenting cells (APCs) in the activation of T cells (25,26), particularly $T_{regs}$ (27,28) in diabetes, CD8$^+$ and CD11b$^+$ conventional dendritic cells, plasmacytoid dendritic cells, and macrophages on day 64 were measured. All dendritic cell subsets within the spleen were increased, but there were no significant changes within the PLN (Supplementary Fig. 5*A*). Macrophages were increased both in the PLN and spleen (Supplementary Fig. 5*B*), consistent with results of previous studies with sRAGE (19).

### Diabetes Prevention by sRAGE Requires $T_{regs}$, and Its Expansion of $T_{regs}$ Is RAGE Dependent

Adoptive transfer of diabetes into NOD/SCID mice (Fig. 2*G*) was performed. Of NOD/SCID recipient mice, 72% and 78% developed diabetes when given either vehicle plus isotype IgG ($T_{reg}$ competent) or vehicle plus anti-FR4 antibodies ($T_{reg}$ deficient), respectively (Fig. 2*H*). None of the NOD/SCID mice treated with sRAGE plus control IgG developed diabetes. However, 56% of those that received sRAGE plus anti-FR4 antibodies to deplete $T_{regs}$ developed diabetes (Fig. 2*H*). There were marked reductions in CD4$^+$CD8$^-$CD25$^+$FoxP3$^+$ $T_{reg}$ proportions in PLNs and spleen of mice treated with anti-FR4 antibodies, whereas sRAGE plus control IgG-treated mice had an increased proportion of $T_{regs}$ in both PLNs and spleen (Fig. 2*I* and *J*).

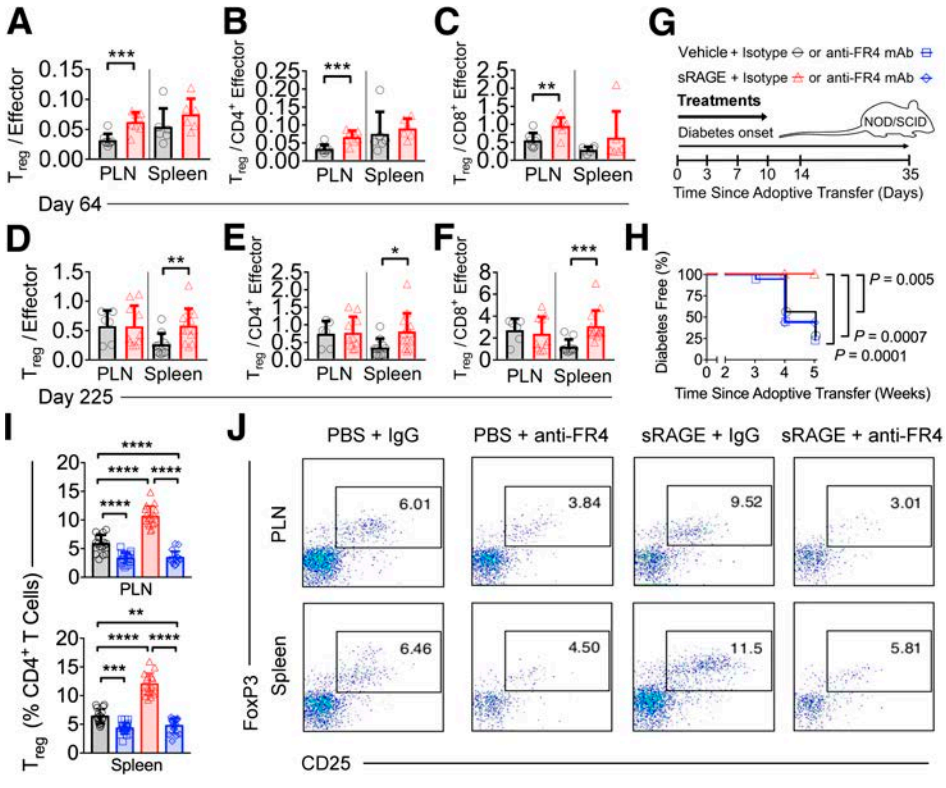


**Figure 2**—$T_{regs}$ are a nonredundant mechanism of action for sRAGE treatment. *A–F*: Flow cytometry quantification of $T_{reg}$-to-$T_{eff}$ ratios on day 64 (*A–C*) and day 225 (*D–F*) in NOD/ShiLt mice ($n$ = 4–13/group). *G*: In an adoptive transfer model of autoimmune diabetes, splenocytes from diabetic NOD/ShiLt donors were adoptively transferred into NOD/SCID recipients. Recipient mice were treated with vehicle or 25 μg sRAGE twice daily for 14 days and isotype control or anti-folate receptor 4 (FR4) monoclonal antibodies (mAb) at 3, 7, 10, and 14 days. Diabetes incidence (three independent experiments, $n$ = 16 mice/group) (*H*) and flow cytometry quantification of $T_{reg}$ frequencies ($n$ = 16 mice/group) (*I* and *J*). *I*: Quantification of frequencies. *J*: Representative dot plots. Column graphs are shown as median (IQR), with analysis with two-tailed Mann-Whitney *U* test. Diabetes incidence is shown with Kaplan-Meier survival curves and was analyzed with log-rank test. *$P < 0.05$; **$P < 0.01$; ***$P < 0.001$; ****$P < 0.0001$.

sRAGE competes for RAGE ligands that are also recognized by other receptors (29), so we investigated the importance of RAGE expression in sRAGE modulation of $T_{regs}$. First, we established that cell-surface RAGE was present on $CD4^+CD8^-CD25^+Foxp3^+$ $T_{regs}$ in the PLN and spleen in NOD/ShiLt mice on day 50 of life (Fig. 3*A* and *B*), at the commencement of sRAGE treatment. Then, using the C57BL/6 mouse as a model organism (in which $T_{reg}$ RAGE expression was comparable with NODs in the spleen and PLN) (Fig. 3*B*), we administered sRAGE to wild-type or RAGE KO mice from day 50 to 64 of life (Fig. 3*C*). Consistent with our findings in NOD/ShiLt mice, there was a significant increase in the $T_{reg}$-to-$T_{eff}$ ratios in both the PLN and spleen of C57BL/6 mice administered sRAGE (Fig. 3*D*). However, sRAGE treatment in RAGE KO mice did not alter $T_{reg}$-to-$T_{eff}$ cell ratios in these lymphoid tissues (Fig. 3*E*).

We interrogated expression of the proliferation marker Ki67, as well as $T_{reg}$ activation markers TIGIT, KLRG1, CD44, and CD62L (representative histograms and dot plots shown in Fig. 3*F*) in the PLN and spleen of both wild-type and RAGE KO mice administered sRAGE. Consistent with the elevated $T_{reg}$-to-$T_{eff}$ ratios, the proportion of $CD4^+CD8^-CD25^+Foxp3^+$ $T_{regs}$ expressing the proliferation marker Ki67 in wild-type mice had increased after sRAGE treatment, whereas $CD4^+CD8^-Foxp3^-$ $T_{conv}$ expression of Ki67 had declined (Fig. 3*G*). $T_{reg}$ TIGIT and KLRG1 expression was also greater following sRAGE administration in C57BL/6 mice (Fig. 3*G*), indicating the presence of activated and highly proliferative $T_{regs}$ (30). sRAGE-treated $T_{regs}$ in wild-type mice also presented a more activated phenotype, with a reduced proportion of $CD62L^+CD44^-$ naive $T_{regs}$ and an increased proportion of $CD62L^-CD44^+$ effector and $CD62L^+CD44^+$ memory $T_{regs}$ (Fig. 3*G*). The expression of Ki67, TIGIT, KLRG1, CD62L, and CD44 was unchanged in the RAGE KO cohort following sRAGE therapy (Fig. 3*H*).

### Targeted Reduction of AGEs by sRAGE

On day 64, immediately after sRAGE treatment, there were no changes to the circulating concentrations of RAGE ligands, including the AGEs (31,32), CML, CEL, or MG-H1 (Table 1). There were also no differences in the circulating AGE precursors methylglyoxal, glyoxal, or 3-deoxyglucosone (Table 1). However, by day 225 all plasma AGE concentrations were decreased in the sRAGE-treated group (vs. vehicle) (Table 1). Plasma concentrations of other RAGE ligands, S100A8, S100A9, S100B, and HMGB1, did not differ between sRAGE and vehicle groups at any time (Table 1).

### Islet Insulin and $T_{reg}$ Proportions Are Increased After sRAGE Treatment

We hypothesized that sRAGE could also increase the proportion of $T_{regs}$ within pancreatic islets, thereby providing local immunoregulation and a direct improvement in insulin expression. $CD3^+CD4^+FoxP3^+$ $T_{reg}$ proportions were increased on both day 64 and day 225 in the islets of sRAGE-treated mice (Fig. 4*A* and *C*). Similarly, we observed higher islet insulin expression on day 64 immediately following cessation of sRAGE treatment (Fig. 4*B* and *C*), and this persisted to day 225 in sRAGE-treated mice (Fig. 4*B* and *C*). These improvements in insulin expression were significantly correlated with the proportion of islet $T_{regs}$ (Fig. 4*D*), suggesting that local islet $T_{reg}$ modulation could improve insulin expression.

Finally, we performed OGTTs to assess functional improvements. The changes in oral glucose tolerance emerged gradually, with no differences in glucose concentrations or insulin secretion on day 64 (Supplementary Fig. 6*A*–*E*). On day 80, sRAGE-treated mice had increased blood glucose concentrations at 120 min (Supplementary Fig. 6*F*). However, the glucose area under the curve ($AUC_{glucose}$) remained unchanged (Supplementary Fig. 6*G*). Importantly, the insulin area under the curve ($AUC_{insulin}$) had increased in sRAGE-treated mice (Fig. 4*E* and Supplementary Fig. 6*H*), suggesting an overall increase in insulin secretion. There was a tendency toward increased insulin sensitivity ($AUC_{glucose}$–to–$AUC_{insulin}$ ratio), but this did not reach statistical significance (Fig. 4*F*) ($P = 0.08$).

On day 225, in mice that responded to sRAGE treatment and did not progress to diabetes, functional improvements in oral glucose tolerance were evident, including a marked decrease in glucose concentrations during OGTT and improved insulin sensitivity (Fig. 4*G*–*I*). Specifically, sRAGE mice had lower blood glucose concentrations at 0 and 15 min (vs. vehicle) (Fig. 4*G*) that declined by 60 and 120 min (vs. 15- and 30-min time points in the sRAGE group) (Fig. 4*G*), which was not seen in the control mice. In addition, $AUC_{glucose}$ trended toward an improvement (Fig. 4*H*) ($P = 0.06$). While plasma insulin and $AUC_{insulin}$ were unchanged between groups at day 225 (Supplementary Fig. 6*I* and *J*), the $AUC_{glucose}$–to–$AUC_{insulin}$ ratio was decreased in sRAGE mice (Fig. 4*I*), consistent with a long-term improvement in insulin sensitivity.

### sRAGE Promotes the Proliferation of Functional Human $nT_{regs}$ in Coculture

Plasma RAGE ligands, AGEs, are independent predictors for T1D development in humans (33), and sRAGE treatment decreased circulating AGEs by the study end (Table 1). Therefore, we tested whether AGEs directly bind human $T_{regs}$, influencing their proliferation and function. Fresh $CD3^+CD4^+CD25^+CD127^{lo/-}$ human $T_{regs}$ (Supplementary Fig. 7*A* and *B*), of which 90.2 ± 7.1% were positive for FoxP3 (Supplementary Fig. 7*C* and *D*), were incubated with fluorescently labeled AGEs, which time dependently increased cellular fluorescent intensity (Fig. 5*A*). This was abrogated by coadministration of neutralizing anti-RAGE antibodies (Fig. 5*A*) and significantly lower in human $T_{regs}$ incubated with control fluorescently labeled HSA (Fig. 5*A*).

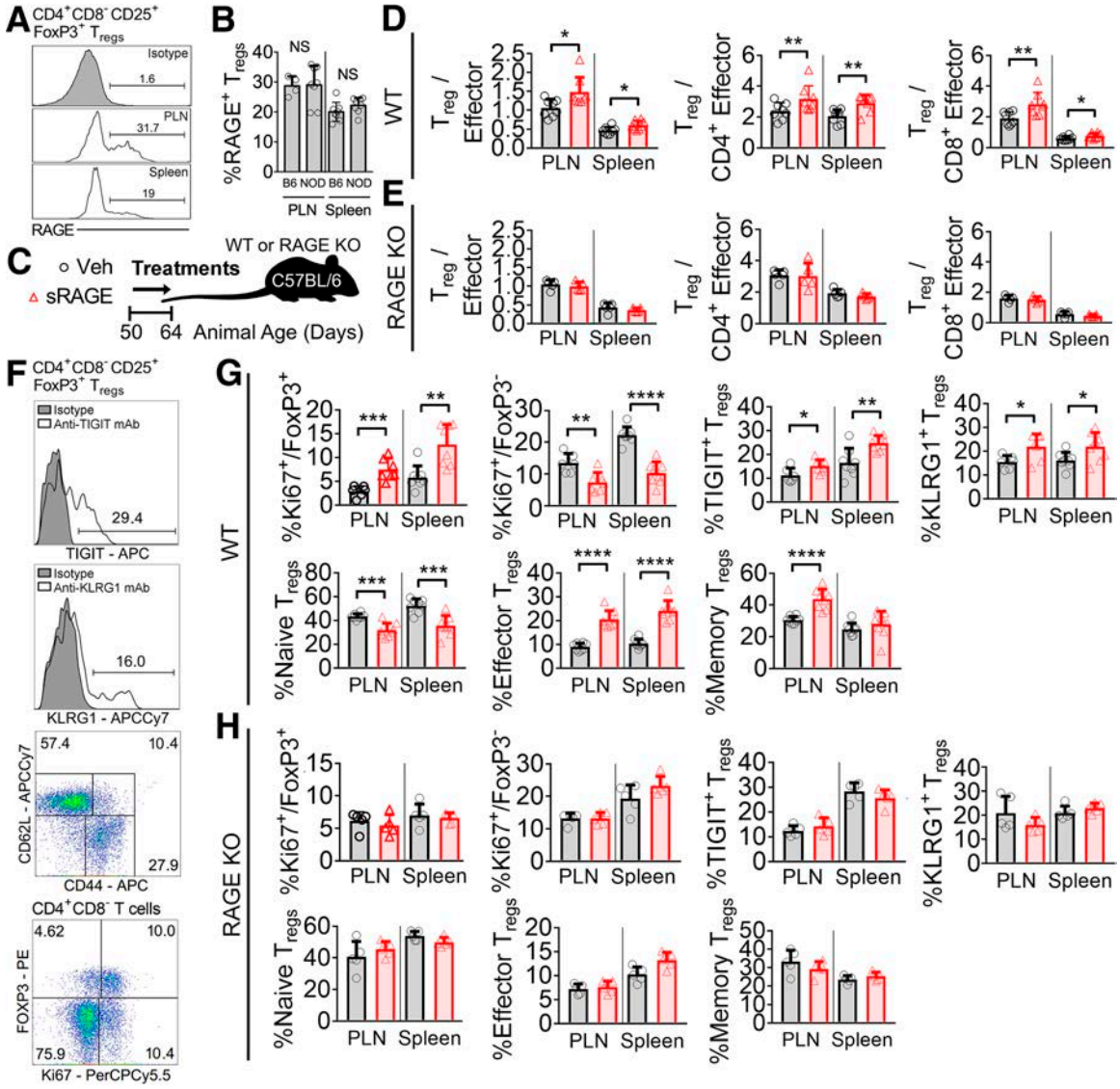


**Figure 3**—RAGE is required for the modulation of $T_{reg}$-to-$T_{eff}$ ratios by sRAGE treatment. *A* and *B*: Flow cytometry quantification of RAGE expression on $CD4^+CD8^-CD25^+FoxP3^+$ $T_{regs}$ in a mouse model of autoimmune diabetes (NOD/ShiLt) and C57BL/6 mice on day 50 of life. *A*: Representative histograms. *B*: Proportion of $RAGE^+$ $T_{regs}$ ($n$ = 4–8 mice/tissue). *C*: Wild-type and RAGE KO C57BL/6 mice were administered vehicle (Veh) (black bars/circles) or treated with 25 μg sRAGE twice daily (red bars/triangles) on day 50–64 of life. *D* and *E*: $T_{reg}$-to-$T_{eff}$ ratios on day 64 in wild-type (WT) (*D*) and RAGE KO (*E*) mice ($n$ = 8 mice/group). *F–H*: TIGIT, KLRG1, CD62L, CD44, and Ki67 expression. *F*: Representative histograms and gating strategies. *G*: Wild-type mice. *H*: RAGE KO mice. Column graphs are shown as means ± SD, with analysis with two-tailed Student $t$ test. *$P$<0.05; **$P$ < 0.01; ***$P$ < 0.001; ****$P$ < 0.0001. mAb, monoclonal antibody; NS, not significant; PE, phycoerythrin.

Next, fresh human $CD3^+CD4^+CD25^+CD127^{lo/-}$ $nT_{regs}$ and $CD3^+CD4^+CD25^-$ $T_{convs}$ were cocultured (Supplementary Fig. 7) following labeling with CFSE or CellTrace Violet, respectively, in the presence of the RAGE ligand AGEs, with or without sRAGE treatment (Fig. 5*B*). Here, sRAGE accelerated $nT_{reg}$ proliferation while decreasing the proliferation index of $T_{convs}$ (Fig. 5*B–D*). These effects occurred through PI3K-Akt-mTOR signaling, as the addition of inhibitors for this pathway (wortmannin and triciribine) dose dependently quenched $nT_{reg}$ proliferation (Fig. 5*B–D*) (34). Similarly, the proliferation of sRAGE-treated $T_{conv}$ cells decreased in the presence of wortmannin and triciribine (Fig. 5*B–D*).

We also tested whether sRAGE could promote the generation of $iT_{regs}$. Here, $CD3^+CD4^+CD45RA^+CD45RO^-$ naive human T cells were isolated (Supplementary Fig. 8*A* and *B*), stimulated as previously described (23) in the presence of AGEs, and analyzed for $iT_{reg}$ differentiation (Supplementary Fig. 8*C–E*). Under these conditions, sRAGE treatment modestly decreased $iT_{reg}$ generation (Supplementary Fig. 9*A* and *B*), suggesting that $iT_{regs}$ do not contribute to increases in the overall population of $T_{regs}$ after sRAGE treatment.

**Table 1—Plasma concentrations of RAGE ligands in NOD/ShiLt mice**

| | Day 64 of life | | Day 225 of life | |
|---|---|---|---|---|
| Treatment | Vehicle | sRAGE | Vehicle | sRAGE |
| CML (nmol/mmol Lys) | 32.2 (3.5) | 31.1 (3.7) | 76.5 (10.6) | 71.1 (12.4)* |
| CEL (nmol/mmol Lys) | 13.5 (4.0) | 16.2 (8.0) | 15.4 (3.8) | 12.3 (4.2)* |
| MG-H1 (nmol/mmol Lys) | 229.3 (45.1) | 260.1 (56.4) | 267.7 (39.5) | 247.0 (54.6)* |
| MGO (nmol/L) | 499.5 (78.8) | 436.4 (142.9) | 643.7 (280.2) | 556.1 (246.4) |
| GO (nmol/L) | 848.4 (301.8) | 958.3 (316.0) | 1,083.0 (505.2) | 1,004.0 (518.5) |
| 3-DG (nmol/L) | 987.3 (254.7) | 1,163.0 (401.0) | 2,547.0 (476.0) | 2,227.0 (483.0) |
| S100A8 (ng/mL) | 0.5 (0.1) | 7.1 (23.0) | 5.3 (13.1) | 5.0 (26.0) |
| S100A9 (ng/mL) | 166.8 (131.8) | 301.3 (303.0) | 74.9 (144.3) | 100.5 (81.8) |
| S100B (ng/mL) | 1,081.0 (812.9) | 882.5 (512.7) | 1,052.0 (528.8) | 1,077.0 (545.6) |
| HMGB1 (ng/mL) | 11.9 (7.5) | 15.8 (8.2) | 7.1 (3.7) | 5.7 (5.0) |

Data shown as median (IQR), with analysis with two-tailed Mann-Whitney *U* test. $n$ = 12–15/group. 3-DG, 3-deoxyglucosone; GO, glyoxal; Lys, lysine; MGO, methylglyoxal. *$P < 0.05$ vs. vehicle at same time point.

### AGEs Promote Human $nT_{reg}$ Proliferation in Monoculture but Inhibit Suppressive Function

In $nT_{reg}$ monoculture experiments in the presence of AGEs (Fig. 5*E*), sRAGE increased the mean fluorescence intensity of CFSE-labeled $nT_{regs}$ (vs. vehicle) (Fig. 5*E* and *F*) when other T-cell populations were absent. This is consistent with a previous observation that RAGE silencing in human T cells decreased responsiveness to costimulation and proliferation (35).

However, in $nT_{regs}$, proliferation can be associated with a loss of suppressive function (22,36). Hence, AGEs could induce $nT_{reg}$ proliferation but, in the absence of other T-cell populations, may limit their function. For testing this, human $nT_{reg}$ monoculture experiments examined changes in gene expression with use of NanoString. PCA distinctively separated the HSA-treated (control) and AGE-HSA–treated $nT_{regs}$ (Fig. 6*A*), where principal component 1 accounted for 56% of the overall variance. HSA-treated $nT_{regs}$ were enriched in the expression of genes involved in $nT_{reg}$ function (*JAK1*, *IRF4*, *SOCS1*) (Fig. 6*A*) (37–39) as compared with AGE-HSA–treated $nT_{regs}$.

Differentially expressed genes were visualized by volcano plot (Fig. 6*B*) where AGE-treated $nT_{regs}$ had reduced expression of key $nT_{reg}$ genes including *FOXP3*, *IL7R*, *TIGIT*, and *STAT5b* (40) and genes promoting $nT_{reg}$ function (*BACH2*, *CD96*, *IL10RA*, *JAK1/3*, *ITK*, *CD27*, *IRF4*, *STAT3/6*, *CD226*) (30,37,39,41–47) and migration (*CCR4*, *AHR*) (35,48). AGE-treated $nT_{regs}$ also had changes in granzymes A/B/K and granulysin (*GZMB*, *GZMB*, *GZMK*, *GNLY*) and decreased expression of *EOMES* (Fig. 6*B*), a marker for T-cell exhaustion.

Pathway enrichment analysis of genes downregulated by AGEs identified significant biological pathways including interleukin-2 and -7 family signaling, JAK/STAT signaling, and the PDGF/EGFR signaling pathways (Fig. 6*C*), which maintain $nT_{reg}$ function (49,50). Ingenuity Pathway Analysis predicted 161 upstream regulators of AGE-induced changes (Fig. 6*D* and Supplementary Table 1) including $nT_{reg}$ signaling molecules (*CD28*, *IL2*, *CD3*, *STAT3*, *TCR*) and other T cell–associated proteins (*IL4*, *TBX21*, *NPC2*, *CEBPB*, *GATA3*) (Fig. 6*D*). Finally, network analysis–identified (Supplementary Table 2) neighboring nodes for *FOXP3* and several genes upstream (*IL10RA*, *STAT3/5B*, *NFATC2*) and downstream (*IL7R*, *CCR4*) of *FOXP3* changed in response to AGE exposure (Fig. 6*E*). Predicted upstream regulators after AGE treatment (*CD3*, *TCR*) (Fig. 6*D*) were also neighboring nodes of *FOXP3* (Fig. 6*E*). All other genes were either two or three nodes adjacent to *FOXP3* (Fig. 6*E*), highlighting the intimate cross talk among genes impacted by AGEs and the $nT_{reg}$ master regulatory gene *FOXP3*.

## DISCUSSION

There is an urgent unmet need for novel disease targets and therapies that are reproducible and have high potential for translation to prevent T1D in humans (7). Here, we report that a decoy RAGE (sRAGE), which may act to antagonize cellular RAGE signaling, has a novel immunomodulatory role that contributes to the balance between $T_{regs}$ and $T_{effs}$, a critical process in self-tolerance (3). sRAGE therapy in several murine models increased $T_{reg}$ ratios in lymphoid tissues such as PLN and spleen (24) and within pancreatic islet immune cell infiltrates. In human T-cell culture, sRAGE promoted expansion of functional human $nT_{regs}$, whereas the RAGE ligands AGEs significantly impaired $nT_{reg}$ suppressive function. Ultimately, we showed that short-term intervention with sRAGE restored $T_{reg}$-to-$T_{eff}$ ratios, protecting against diabetes onset at two independent research centers.

Immediately after sRAGE therapy on day 64, islet infiltration was reduced, accompanied by increases in the absolute numbers of $T_{regs}$ as well as $T_{reg}$-to-$T_{eff}$ ratios in the PLN. These immediate but transient changes in local $T_{regs}$ in the PLN (19), supported by increased islet $T_{reg}$

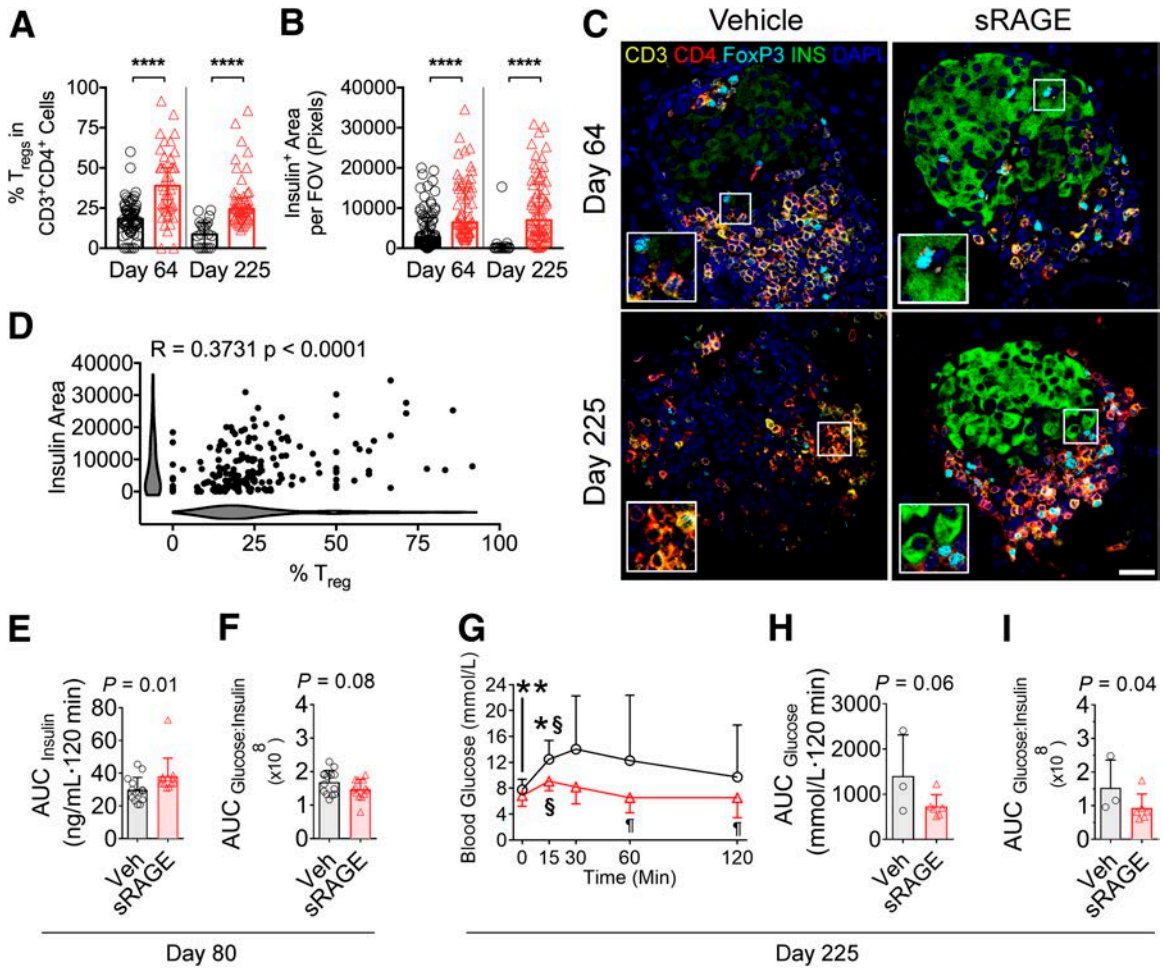


**Figure 4**—Improvements in islet-infiltrating $T_{regs}$, insulin expression, and oral glucose tolerance following sRAGE treatment in NOD/ShiLt mice. *A–D*: Multiplexed immunofluorescence staining and quantification of CD3, CD4, FoxP3, insulin, and DAPI ($n$ = 10–20 sections/mouse from $n$ = 6 mice/group). Inset images are ×2 magnified. *A*: Proportion of islet-infiltrating $CD3^+CD4^+FoxP3^+$ $T_{regs}$. *B*: Insulin area per field of view (FOV). *C*: Representative photomicrographs. Bar, 40 μm. *D*: Correlation analyses of $CD3^+CD4^+FoxP3^+$ $T_{reg}$ proportions and insulin area (shaded bars are Kernel plots showing variable distribution). *E–I*: OGTTs on day 80 ($n$ = 15/group) and 225 ($n$ = 3–6/group) of life. *E*: Day 80 $AUC_{insulin}$. *F*: Day 80 $AUC_{glucose}$–to–$AUC_{insulin}$ ratios. *G*: Day 225 blood glucose concentrations. *H*: Day 225 $AUC_{glucose}$. *I*: Day 225 $AUC_{glucose}$–to–$AUC_{insulin}$ ratio. Data shown as means ± SD and were analyzed with two-tailed unpaired or paired Student $t$ tests. Correlation analyses were performed with Spearman test. *$P < 0.05$ between groups; **$P < 0.01$ between groups; ****$P < 0.0001$ between groups; §$P < 0.05$ vs. 0 min within the same group; ¶$P < 0.05$ vs. 15- and 30-min time points within the same group. Veh, vehicle.

infiltration, are likely critical for islet preservation and act to suppress the priming of autoantigen-specific T cells in the early stages of T1D (24). By contrast, modulation of PLN T cells has been reported as less critical in the later stages of T1D disease progression (51). Depletion of $T_{regs}$ specifically showed that these cells were essential for the protection afforded against diabetes by sRAGE. Further, we verified these effects of sRAGE on human $T_{regs}$. $T_{reg}$ immunomodulation comparable with that seen with sRAGE is being considered in other interventions that are lead candidates for the treatment of T1D (52).

Importantly, improved β-cell function as assessed with OGTT after sRAGE treatment emerged on day 80 and was preceded by the immediate changes on day 64 in the islets including increased $T_{reg}$ infiltration and insulin expression. These improvements in glucose tolerance persisted to day 225 in mice that responded to sRAGE treatment and did not progress to diabetes, resulting in an improvement in insulin sensitivity and a preservation of islet numbers, which is consistent with the long-lasting protection afforded against diabetes (53).

Mice deficient in RAGE (RAGE KO) did not have increased $T_{reg}$-to-$T_{eff}$ cell ratios within lymphoid tissues following sRAGE administration, alluding to the importance of cellular RAGE antagonism as a mechanism of this therapy. Certainly, there is increasing investigation into strategies to decrease RAGE ligands for the modulation of autoimmune diabetes risk in mice (31,32,54–56), and the RAGE ligand CML is a known risk factor for T1D onset in humans (33). It is particularly interesting that in prior studies investigators have found RAGE ligand inhibition can have direct effects on the islets in the context of T1D

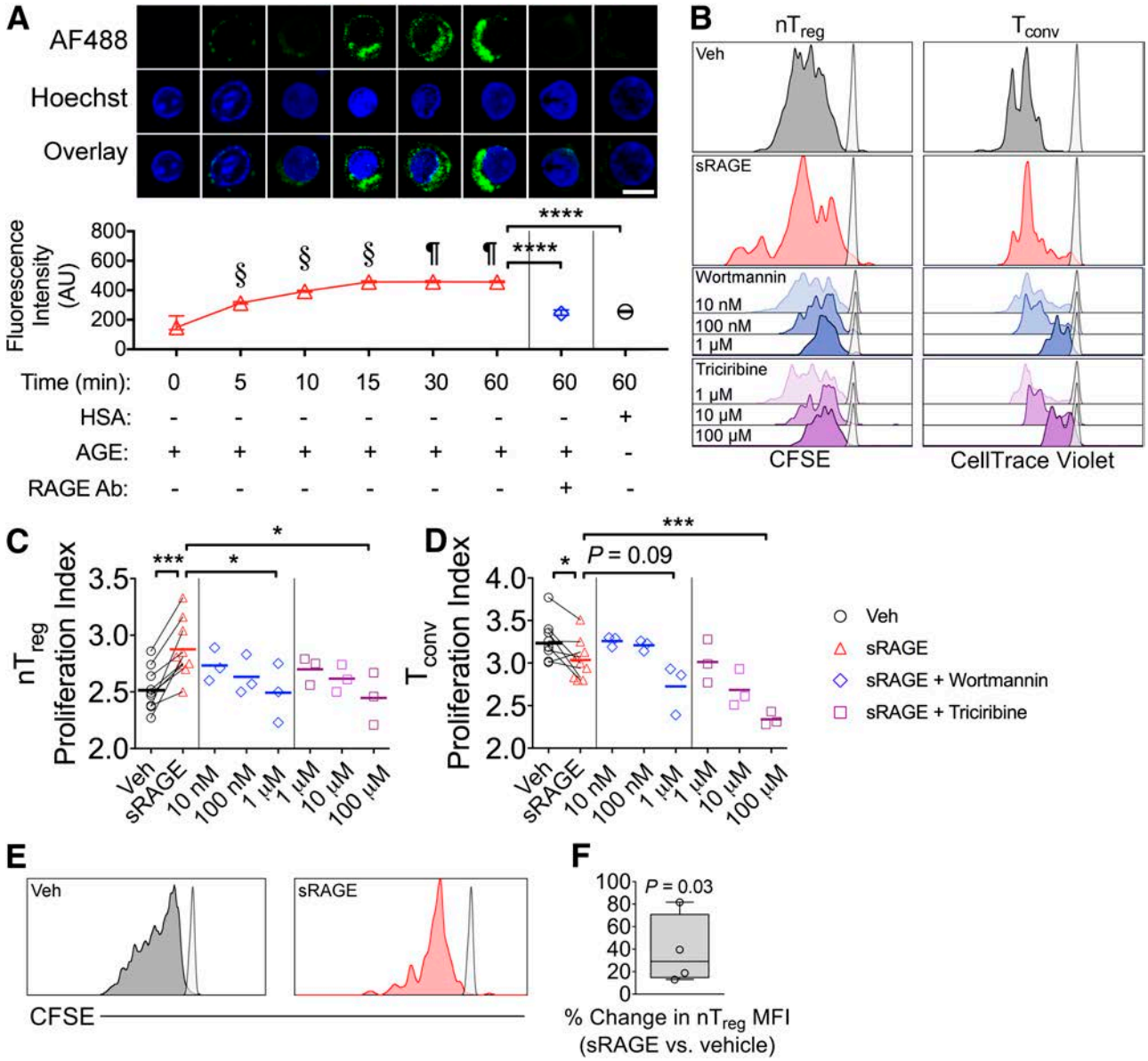


**Figure 5**—Human nT$_{regs}$ bind AGEs in a RAGE-dependent manner and proliferate more in coculture when treated with sRAGE. *A*: Human CD3$^+$CD4$^+$CD25$^+$CD127$^{lo/-}$ nT$_{regs}$ were incubated with AGE-modified HSA (AGE-HSA or AGE) or unmodified HSA (HSA)—both labelled with Alexa Fluor 488 (AF488). Anti-RAGE antibody (Ab) was added to the culture as indicated. Bar, 10 μm. $n$ = 3 donors/group. *B–D*: CFSE-labeled CD3$^+$CD4$^+$CD25$^+$CD127$^{lo/-}$ nT$_{regs}$ and CellTrace Violet–labeled CD3$^+$CD4$^+$CD25$^-$ T$_{convs}$ were stimulated in 3-day coculture at a 1:1 ratio containing anti-CD3/CD28 MACSiBeads (1:10 bead:cell ratio). *B*: Representative histograms (unstimulated controls presented as semi-transparent peaks). *C–D*: Proliferation indices of nT$_{regs}$ and T$_{convs}$ when administered vehicle or 50 μg sRAGE daily ($n$ = 9/group), as well as sRAGE in addition to PI3K-Akt-mTOR pathway inhibitor wortmannin or triciribine ($n$ = 3/group). *E* and *F*: CFSE-labeled CD3$^+$CD4$^+$CD25$^+$CD127$^{lo/-}$ nT$_{regs}$ were stimulated in 3-day monoculture containing anti-CD3/CD28 MACSiBeads (1:20 bead:cell) and 200 IU/mL IL-2. *E*: Representative histograms. *F*: Percent change in CFSE mean fluorescence intensity (MFI) ($n$ = 4/group). Data are shown as mean ± SD, with analysis with paired two-tailed Student $t$ tests. §$P < 0.05$ vs. all previous time points. ¶$P < 0.05$ vs. 0, 5, 10, and 15 min. *$P < 0.05$; ***$P < 0.001$; ****$P < 0.0001$. AU, arbitrary units; Veh, vehicle.

(32,54). RAGE plays an important role in T-cell survival (13) and proliferation (35), including in individuals at risk for T1D, but whether this applied to specific T-cell subsets, such as T$_{regs}$, remained unknown. In the current study, we confirm that RAGE ligands could modulate human T-cell function and the expression of RAGE on T$_{regs}$ in the PLN and spleen of NOD/ShiLt mice was required for sRAGE treatment to improve localized T$_{reg}$-to-T$_{eff}$ ratios after therapy completion.

However, elevations in circulating RAGE ligands termed AGEs, including CML, CEL, and MG-H1, were not evident in this study until day 225 of life, and this was substantially improved by sRAGE treatment. This is unsurprisingly consistent with improvements in longer-term glucose

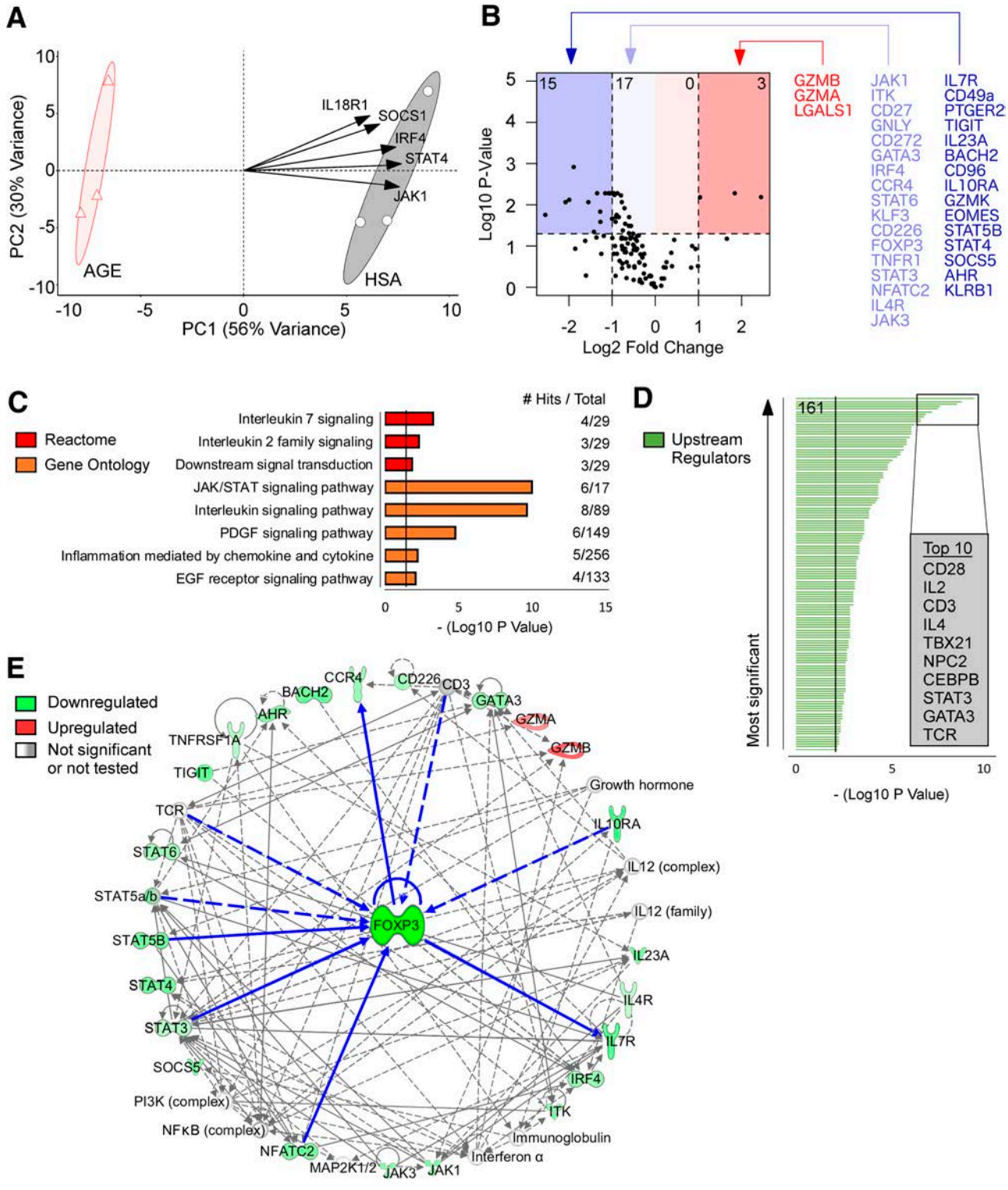


**Figure 6**—AGE treatment of human $nT_{regs}$ downregulates key genes for suppressive function and manipulates signaling cascades upstream and downstream of *FOXP3*. *A*: PCA with the top five variable loadings shown as arrows. *B*: Volcano plot visualization for changes in gene expression (number of differentially expressed genes shown in top corners). *C*: Pathway enrichment analysis with use of the Reactome and Gene Ontology databases. *D*: Upstream regulator predictions with use of Ingenuity Pathway Analysis (161 significant regulators were identified). *E*: Network analysis with *FOXP3* as the focus node. Neighboring molecules are connected to *FOXP3* with bolded blue lines. All other molecules are two to three nodes adjacent to *FOXP3*. Direct relationships are shown as solid lines, and indirect relationships are shown as dashed lines. $n = 3$/group. *P* values were corrected with false discovery rate or Bonferroni adjustment. PC1, principal component 1.

control seen in these mice, given that the widely used clinical markers for glucose control, $HbA_{1c}$, glycated albumin, and fructosamine, are in fact AGEs/AGE precursors. As alluded to above, there is also evidence that increased circulating AGEs in children are an independent risk factor for T1D onset (23), supported by the protection afforded against T1D by sRAGE therapy. An essential future direction of this work would be to mutate the RAGE ligand binding domain of sRAGE to assess whether this negates its protection against T1D. Indeed, in previous work in murine models of atherosclerosis investigators found that the nonligand binding domains of sRAGE can inhibit G-protein–coupled receptors to alleviate inflammation (53). Therefore, there is likely potential for additional non-RAGE ligand–related benefits of the sRAGE protein.

AGEs promoted human $nT_{reg}$ proliferation when these cells were cultured alone, but they significantly impaired $nT_{reg}$ function. By contrast, sRAGE treatment expanded functional human $nT_{regs}$ by increasing the proliferation of $nT_{regs}$ that could inhibit $T_{conv}$ cell division in coculture. Similarly, in addition to increased $T_{reg}$-to-$T_{eff}$ ratios seen in the NOD murine models, sRAGE increased the expression of the $T_{reg}$ activation markers Ki67, TIGIT, KLRG1, and CD44 in wild-type C57BL/6 but not RAGE KO mice. It was noteworthy that RAGE KO mice did not have changes in $T_{reg}$-to-$T_{eff}$ ratios compared with wild-type mice prior to sRAGE treatment. However, as alluded to in this study, the function of T cells and $T_{regs}$ in mice with complete RAGE KO may be compromised.

There are limitations to this study. Further studies are required to optimize the dosing regimen and therapeutic window for sRAGE. In support of this, a few subclinical hallmarks of diabetes remained present in sRAGE-treated mice that did not progress to diabetes, which suggests titration may further improve treatment efficacy. These included a residual level of islet infiltration and suboptimal first-phase insulin release following an oral glucose challenge at the study end in nonprogressing mice. In addition, since sRAGE is a biologic, it is important to develop effective administration methods to achieve circulating concentrations in humans that can reproduce the efficacious effects in mice. Although recombinant human sRAGE is unlikely to be immunogenic, given it is an endogenous human protein, it would be worthwhile to investigate whether RAGE-specific autoantibodies are produced as a result of this treatment. Further characterization of the T-cell effects of sRAGE would also be worthwhile, including tetramer-based assays of antigen-specific T cells, using T cells from patients at risk for T1D and patients with T1D and replicating the human T-cell studies across a wider range of $T_{reg}$-to-$T_{conv}$ ratios to assess the robustness of sRAGE treatment across physiologically varied ratios of these immune cells. Future research could also investigate the effects of sRAGE treatment on APC function, given its ability to increase macrophage and dendritic cell numbers, as well as its effects on B cells as an APC and specialized subsets such as T regulatory type 1 (TR1) cells.

In summary, we have shown that sRAGE is a biologic that can modulate $T_{reg}$ responses, including through the RAGE ligand AGEs. This was ascertained with human T-cell assays as well as use of murine models that were RAGE deficient or at high risk of autoimmune diabetes, where the presence of functional $T_{regs}$ is known to be compromised. We showed that a short-term 2-week intervention with sRAGE elicited persistent effects on the immune system, ultimately preserving β-cell function and reducing diabetes incidence in a multisite preclinical trial. Given that sRAGE is a native protein that is reduced in children at risk for T1D, and has persistent benefits on insulin expression, oral glucose tolerance, and $T_{reg}$-to-$T_{eff}$ ratios, we suggest that this treatment is a promising new therapy for further development to prevent T1D.

**Acknowledgments.** The authors thank I. Rojas and S. Diaz-Guilas (Mater Research ) for assistance with the human T-cell studies; C. O'Brien and T. Friesen (Type 1 Diabetes Research Center, Novo Nordisk) for assistance with the diabetes incidence study at site 2; I. Buckle, J. Naranjo, and E. Hamilton-Williams (Diamantina Institute) for providing diabetic NOD mice for the adoptive transfer study; J. Lynch and S. Phipps (The University of Queensland) for providing RAGE KO mice for exploratory analyses; K. MacDonald (Queensland Institute for Medical Research Berghofer) for advice on $T_{reg}$ studies; E. Williams and the Australian Equine Genetics Research Centre (The University of Queensland) for advice with the RAGE KO mice; and the Biological Resources, Flow Cytometry, Histology, and Microscopy facilities at the Translational Research Institute for their operational assets and expert guidance.

**Funding.** This work was supported by the NHMRC (1023661), JDRF (5-2010-163), Diabetes Australia, the Victorian Government Infrastructure Program, and Mater Foundation. S.S.L. was supported by the Research Training Program and JDRF, A.K.F. and N.F. by the Research Training Program, A.Z. by Kidney Health Australia, R.J.S. by an Australian Research Council fellowship (FT110100372), and J.M.F. by NHMRC fellowships (1004503, 1102935).

**Duality of Interest.** P.-H.G. is a board member of AbbVie, AstraZeneca, Boehringer Ingelheim, Cebix, Eli Lilly, Janssen, Medscape, Novartis, Novo Nordisk, and Sanofi. P.-H.G. received lecture honoraria from AstraZeneca, Boehringer Ingelheim, Eli Lilly, Genzyme, Merck Sharp & Dohme, Novartis, Novo Nordisk, and Sanofi. P.-H.G. received grants from Eli Lilly and Roche. M.K. is a board member and minor (<5%) shareholder of Vactech Ltd. M.K. received lecture honoraria from Novo Nordisk. T.E.B. and J.C. received income and research support from Novo Nordisk. No other potential conflicts of interest relevant to this article were reported.

**Author Contributions.** S.S.L. designed and performed experiments, analyzed and interpreted data, and prepared the manuscript. D.J.B., D.A.M., A.Z., A.K.F., N.F., T.W., J.J.M., J.L.S., and C.G.S. performed experiments. T.E.B. designed and J.C. performed the incidence experiment at the second site, and both completed its data analyses and interpretation. K.J.R. assisted with the human study design and completion. P.-H.G., R.J.S., and M.K., led by J.M.F., conceptualized and designed the overall study, gained financial support, and completed data analyses and interpretation. All authors edited and approved the final manuscript. S.S.L. and J.M.F. are the guarantors of this work and, as such, had full access to all the data in the study and take responsibility for the integrity of the data and the accuracy of the data analysis.

**Prior Presentation.** Parts of this study were presented in abstract form at the 75th Scientific Sessions of the American Diabetes Association, Boston, MA, 5–9 June 2015.

## References


1. Atkinson MA, Eisenbarth GS, Michels AW. Type 1 diabetes. Lancet 2014; 383:69–82
2. Tao B, Pietropaolo M, Atkinson M, Schatz D, Taylor D. Estimating the cost of type 1 diabetes in the U.S.: a propensity score matching method. PLoS One 2010;5:e11501
3. Brusko TM, Wasserfall CH, Clare-Salzler MJ, Schatz DA, Atkinson MA. Functional defects and the influence of age on the frequency of CD4+ CD25+ T-cells in type 1 diabetes. Diabetes 2005;54:1407–1414
4. Laban S, Suwandi JS, van Unen V, et al. Heterogeneity of circulating CD8 T-cells specific to islet, neo-antigen and virus in patients with type 1 diabetes mellitus. PLoS One 2018;13:e0200818
5. Rosenzwajg M, Churlaud G, Mallone R, et al. Low-dose interleukin-2 fosters a dose-dependent regulatory T cell tuned milieu in T1D patients. J Autoimmun 2015;58:48–58
6. Alhadj Ali M, Liu YF, Arif S, et al. Metabolic and immune effects of immunotherapy with proinsulin peptide in human new-onset type 1 diabetes. Sci Transl Med 2017;9:eaaf7779
7. Insel RA, Dunne JL, Atkinson MA, et al. Staging presymptomatic type 1 diabetes: a scientific statement of JDRF, the Endocrine Society, and the American Diabetes Association. Diabetes Care 2015;38:1964–1974
8. Herold KC, Bundy BN, Long SA, et al.; Type 1 Diabetes TrialNet Study Group. An anti-CD3 antibody, teplizumab, in relatives at risk for type 1 diabetes. N Engl J Med 2019;381:603–613
9. Leung SS, Forbes JM, Borg DJ. Receptor for advanced glycation end products (RAGE) in type 1 diabetes pathogenesis. Curr Diab Rep 2016;16:100
10. Salonen KM, Ryhänen SJ, Forbes JM, et al. A drop in the circulating concentrations of soluble receptor for advanced glycation end products is associated with seroconversion to autoantibody positivity but not with subsequent progression to clinical disease in children en route to type 1 diabetes. Diabetes Metab Res Rev 2017;33
11. Salonen KM, Ryhänen SJ, Forbes JM, et al. Decrease in circulating concentrations of soluble receptors for advanced glycation end products at the time of seroconversion to autoantibody positivity in children with prediabetes. Diabetes Care 2015;38:665–670
12. Salonen KM, Ryhänen SJ, Forbes JM, et al.; Finnish Pediatric Diabetes Register. Circulating concentrations of soluble receptor for AGE are associated with age and AGER gene polymorphisms in children with newly diagnosed type 1 diabetes. Diabetes Care 2014;37:1975–1981
13. Durning SP, Preston-Hurlburt P, Clark PR, Xu D; Type 1 Diabetes TrialNet Study Group. The receptor for advanced glycation endproducts drives T cell survival and inflammation in type 1 diabetes mellitus. J Immunol 2016;197: 3076–3085
14. Forbes JM, Söderlund J, Yap FY, et al. Receptor for advanced glycation end-products (RAGE) provides a link between genetic susceptibility and environmental factors in type 1 diabetes. Diabetologia 2011;54:1032–1042
15. Liliensiek B, Weigand MA, Bierhaus A, et al. Receptor for advanced glycation end products (RAGE) regulates sepsis but not the adaptive immune response. J Clin Invest 2004;113:1641–1650
16. Leiter EH. The NOD mouse: a model for insulin-dependent diabetes mellitus. Curr Protoc Immunol 2001;Chapter 15:Unit 15.9
17. Yamaguchi T, Hirota K, Nagahama K, et al. Control of immune responses by antigen-specific regulatory T cells expressing the folate receptor. Immunity 2007;27:145–159
18. Borg DJ, Faridi P, Giam KL, et al. Short duration alagebrium chloride therapy prediabetes does not inhibit progression to autoimmune diabetes in an experimental model. Metabolites 2021;11:426
19. Pullerits R, Brisslert M, Jonsson IM, Tarkowski A. Soluble receptor for advanced glycation end products triggers a proinflammatory cytokine cascade via beta2 integrin Mac-1. Arthritis Rheum 2006;54:3898–3907
20. Wang Y, Wang H, Piper MG, et al. sRAGE induces human monocyte survival and differentiation. J Immunol 2010;185:1822–1835
21. Scheijen JL, Schalkwijk CG. Quantification of glyoxal, methylglyoxal and 3-deoxyglucosone in blood and plasma by ultra performance liquid chromatography tandem mass spectrometry: evaluation of blood specimen. Clin Chem Lab Med 2014;52:85–91
22. Putnam AL, Brusko TM, Lee MR, et al. Expansion of human regulatory T-cells from patients with type 1 diabetes. Diabetes 2009;58:652–662
23. Ellis GI, Reneer MC, Vélez-Ortega AC, McCool A, Martí F. Generation of induced regulatory T cells from primary human naïve and memory T cells. J Vis Exp 2012;(62):3738
24. McNally A, Hill GR, Sparwasser T, Thomas R, Steptoe RJ. CD4+CD25+ regulatory T cells control CD8+ T-cell effector differentiation by modulating IL-2 homeostasis. Proc Natl Acad Sci U S A 2011;108:7529–7534
25. Price JD, Beauchamp NM, Rahir G, et al. CD8+ dendritic cell-mediated tolerance of autoreactive CD4+ T cells is deficient in NOD mice and can be corrected by blocking CD40L. J Leukoc Biol 2014;95:325–336
26. Yamazaki S, Dudziak D, Heidkamp GF, et al. CD8+ CD205+ splenic dendritic cells are specialized to induce Foxp3+ regulatory T cells. J Immunol 2008;181: 6923–6933
27. Tordesillas L, Lozano-Ojalvo D, Dunkin D, et al. PDL2$^{+}$ CD11b$^{+}$ dermal dendritic cells capture topical antigen through hair follicles to prime LAP$^{+}$ Tregs. Nat Commun 2018;9:5238
28. Lippens C, Duraes FV, Dubrot J, et al. IDO-orchestrated crosstalk between pDCs and Tregs inhibits autoimmunity. J Autoimmun 2016;75:39–49
29. Das N, Dewan V, Grace PM, et al. HMGB1 activates proinflammatory signaling via TLR5 leading to allodynia. Cell Rep 2016;17:1128–1140
30. Fuhrman CA, Yeh WI, Seay HR, et al. Divergent phenotypes of human regulatory T cells expressing the receptors TIGIT and CD226. J Immunol 2015;195:145–155
31. Borg DJ, Yap FYT, Keshvari S, et al. Perinatal exposure to high dietary advanced glycation end products in transgenic NOD8.3 mice leads to pancreatic beta cell dysfunction. Islets 2018;10:10–24
32. Coughlan MT, Yap FY, Tong DC, et al. Advanced glycation end products are direct modulators of β-cell function. Diabetes 2011;60:2523–2532
33. Beyan H, Riese H, Hawa MI, et al. Glycotoxin and autoantibodies are additive environmentally determined predictors of type 1 diabetes: a twin and population study. Diabetes 2012;61:1192–1198
34. Wang Y, Camirand G, Lin Y, et al. Regulatory T cells require mammalian target of rapamycin signaling to maintain both homeostasis and alloantigen-driven proliferation in lymphocyte-replete mice. J Immunol 2011;186:2809–2818
35. Gobert M, Treilleux I, Bendriss-Vermare N, et al. Regulatory T cells recruited through CCL22/CCR4 are selectively activated in lymphoid infiltrates surrounding primary breast tumors and lead to an adverse clinical outcome. Cancer Res 2009;69:2000–2009
36. Gerriets VA, Kishton RJ, Johnson MO, et al. Foxp3 and Toll-like receptor signaling balance $T_{reg}$ cell anabolic metabolism for suppression. Nat Immunol 2016;17:1459–1466
37. Cretney E, Xin A, Shi W, et al. The transcription factors Blimp-1 and IRF4 jointly control the differentiation and function of effector regulatory T cells. Nat Immunol 2011;12:304–311
38. Takahashi R, Nakatsukasa H, Shiozawa S, Yoshimura A. SOCS1 is a key molecule that prevents regulatory T cell plasticity under inflammatory conditions. J Immunol 2017;199:149–158
39. Kirken RA, Rui H, Malabarba MG, et al. Activation of JAK3, but not JAK1, is critical for IL-2-induced proliferation and STAT5 recruitment by a COOH-terminal region of the IL-2 receptor beta-chain. Cytokine 1995;7: 689–700
40. Cohen AC, Nadeau KC, Tu W, et al. Cutting edge: decreased accumulation and regulatory function of CD4+ CD25(high) T cells in human STAT5b deficiency. J Immunol 2006;177:2770–2774

41. Piédavent-Salomon M, Willing A, Engler JB, et al. Multiple sclerosis associated genetic variants of CD226 impair regulatory T cell function. Brain 2015;138:3263–3274
42. Roychoudhuri R, Hirahara K, Mousavi K, et al. BACH2 represses effector programs to stabilize T(reg)-mediated immune homeostasis. Nature 2013;498:506–510
43. Chaudhry A, Samstein RM, Treuting P, et al. Interleukin-10 signaling in regulatory T cells is required for suppression of Th17 cell-mediated inflammation. Immunity 2011;34:566–578
44. Huang W, Jeong AR, Kannan AK, Huang L, August A. IL-2-inducible T cell kinase tunes T regulatory cell development and is required for suppressive function. J Immunol 2014;193:2267–2272
45. Duggleby RC, Shaw TN, Jarvis LB, Kaur G, Gaston JS. CD27 expression discriminates between regulatory and non-regulatory cells after expansion of human peripheral blood CD4+ CD25+ cells. Immunology 2007;121:129–139
46. Sanchez-Guajardo V, Tanchot C, O'Malley JT, Kaplan MH, Garcia S, Freitas AA. Agonist-driven development of CD4+CD25+Foxp3+ regulatory T cells requires a second signal mediated by Stat6. J Immunol 2007;178:7550–7556
47. Pallandre JR, Brillard E, Créhange G, et al. Role of STAT3 in CD4+CD25+FOXP3+ regulatory lymphocyte generation: implications in graft-versus-host disease and antitumor immunity. J Immunol 2007;179:7593–7604
48. Ye J, Qiu J, Bostick JW, et al. The aryl hydrocarbon receptor preferentially marks and promotes gut regulatory T cells. Cell Rep 2017;21:2277–2290
49. Wang S, Zhang Y, Wang Y, et al. Amphiregulin confers regulatory T cell suppressive function and tumor invasion via the EGFR/GSK-3β/Foxp3 axis. J Biol Chem 2016;291:21085–21095
50. Lo Re S, Lecocq M, Uwambayinema F, et al. Platelet-derived growth factor-producing CD4+ Foxp3+ regulatory T lymphocytes promote lung fibrosis. Am J Respir Crit Care Med 2011;184:1270–1281
51. Gagnerault MC, Luan JJ, Lotton C, Lepault F. Pancreatic lymph nodes are required for priming of beta cell reactive T cells in NOD mice. J Exp Med 2002;196:369–377
52. Sherry N, Hagopian W, Ludvigsson J, et al.; Protégé Trial Investigators. Teplizumab for treatment of type 1 diabetes (Protégé study): 1-year results from a randomised, placebo-controlled trial. Lancet 2011;378:487–497
53. Sosenko JM, Skyler JS, Herold KC; Type 1 Diabetes TrialNet and Diabetes Prevention Trial–Type 1 Study Groups. The metabolic progression to type 1 diabetes as indicated by serial oral glucose tolerance testing in the Diabetes Prevention Trial-type 1. Diabetes 2012;61:1331–1337
54. Han J, Zhong J, Wei W, et al. Extracellular high-mobility group box 1 acts as an innate immune mediator to enhance autoimmune progression and diabetes onset in NOD mice. Diabetes 2008;57:2118–2127
55. Peppa M, He C, Hattori M, McEvoy R, Zheng F, Vlassara H. Fetal or neonatal low-glycotoxin environment prevents autoimmune diabetes in NOD mice. Diabetes 2003;52:1441–1448
56. Zhang J, Chen L, Wang F, et al. Extracellular HMGB1 exacerbates autoimmune progression and recurrence of type 1 diabetes by impairing regulatory T cell stability. Diabetologia 2020;63:987–1001